eXogenous Kalman Filter for State-of-Charge Estimation in Lithium-ion Batteries*

Agus Hasan, Martin Skriver, and Tor Arne Johansen

***Abstract*— This paper presents State-of-Charge (SoC) estimation of lithium-ion batteries using eXogenous Kalman filter (XKF). The state-space equation for the lithium-ion battery is obtained from the equivalent circuit model (ECM). It has linear process equations and a nonlinear output voltage equation. The estimation is done using a cascade of nonlinear observer and a linearized Kalman filter. The method is tested using experimental data of a lithium-ion-phosphate ($LiFePO_4$) battery under dynamic stress test (DST) and federal urban driving schedule (FUDS). The results are compared with existing Kalman filters.**

I. INTRODUCTION

State-of-Charge (SoC) battery estimation is an important component in battery management system (BMS). It monitors the states and parameters of the battery, thus provides instantaneous information regarding when a battery needs to be recharged and allows the BMS to prolong the battery life by preventing it from over-charging or over discharging [1], [2], [3]. The SoC cannot be measured directly and has to be estimated based on measurable variables such as current and voltage. The estimation is usually done by employing mathematical or physical models to describe complex nonlinear dynamic processes arising from thermodynamics, electrode kinetics, and transport phenomena [4].

Lithium-ion battery modeling can be approached in three different ways. The first approach is based on thermal-electrochemical model [5], [6], [7]. The model is derived from the first principles and is written as a system of partial differential equations (PDEs) to describe the physics of the battery. Examples of this approach are the Doyle-Fuller-Newman model [8] and the single particle model (SPM) [9]. This approach can accurately match experimental data but are complex and time consuming to solve. Advanced battery modeling using coupled PDEs-ODEs has received much attention in recent years since the estimation method for this kind of systems has been well established [10], [11], [12], [13]. The second approach is to consider a battery as an equivalent circuit that represents the electrical characteristics of the cell [14]. The model, which was taken from RC equivalent circuit models (ECMs), serves as a proxy model and is written as a system of ordinary differential equations (ODEs). Even though this approach does not accurately capture the physics of the battery at high discharge conditions, it can be solved quickly and used in real-time environments [15]. The last approach is based on data-driven and relies on machine learning algorithms to develop relationships between sensor inputs and output of the battery [16], [17]. This approach usually requires significant experimental data to train the model. In resource-constrained computing platforms like in micro unmanned aerial vehicles (UAVs), the complexity and accuracy of the model should be well balanced [18].

The models for lithium-ion batteries are nonlinear. The nonlinearity comes from the output voltage equation, which is given by a nonlinear function of the SoC [19]. For the lithium-ion SoC estimation, there are two common methods [20]: methods based on filters (stochastic estimation) [21], [22] and methods based on nonlinear observer (deterministic estimation) [23], [24], [25], [26]. The first method is a natural choice since the model and the measurements are subject to noises. Kalman filter can be designed to suppress the noise affecting the battery systems. It has good performance and general applicability. As an example, the time-varying Kalman filter is globally exponentially stable and gives optimal filtering by selection of tuning parameters to match the variances of white measurement noise and process noise. Since the state is unknown, the filters must rely on a linearization of the nonlinear model about a state estimate. The second method usually has strong and often has global stability properties, which make the nonlinear observer has large region of attraction. However, both methods have weaknesses. Nonlinear approximations such as the extended Kalman filter (EKF) linearizes the system about the estimated state trajectories. Therefore, in general it loss of both global stability and optimality. On the other hand, nonlinear observers are designed without optimality objectives considering the presence of unknown measurement errors and process disturbances.

In this paper, we presents the eXogenous Kalman filter (XKF) for lithium-ion batteries SoC estimation. The XKF is a cascade of a global nonlinear observer with the linearized Kalman filter, where the estimate from the nonlinear observer is an exogenous signal used for generating a linearized model to the Kalman filter. The nonlinear observer is used to guarantee the estimate converges to the actual value exponentially, while the time-varying Kalman filter is used since the current and voltage measurements are noisy. It has been shown in [27] that the two-stage nonlinear estimator inherits the global stability property of the nonlinear observer.

*This work was supported by the Free the Drones (FreeD) project and the FRINATEK project Multi-stage global sensor fusion for navigation and the Centre of Autonomous Marine Operations and Systems (NTNU AMOS) at the Norwegian University of Science and Technology (NTNU), project numbers 250725 and 223254 respectively.

[1]A. Hasan and M. Skriver are with Center for Unmanned Aerial Systems, Mærsk McKinney Møller Institute, University of Southern Denmark, Odense, Denmark. T.A. Johansen is with department of Cybernetics Engineering, Norwegian University of Science and Technology, Trondheim, Norway. Corresponding email: agha@mmmi.sdu.dk

This paper is organized as follow. The lithium-ion battery model based on the ECM with 2-RC circuit and Coulomb counting method is presented in section II. Section III contains SoC estimation using the XKF. The evaluation using experimental data from the dynamic stress test (DST) and the federal urban driving schedule (FUDS) are presented in section IV. The last section contains conclusions and future works.

II. LITHIUM-ION BATTERY MODELING

In this section, we present a lithium-ion battery model based on the ECM. In general, the ECM offers low complexity description of the lithium-ion battery dynamics with fewer states and parameters, thus suitable for real-time application. The battery SoC quantifies the usable energy at the present cycle and can be defined as

$$\mathrm{SoC}(t) \quad = \quad \mathrm{SoC}(t_0) - \frac{\int_{t_0}^{t} I(\tau)\mathrm{d}\tau}{Q_c} \tag{1}$$

where I denotes the current, t_0 denotes the initial time, and Q_c is the nominal capacity. Calculating the SoC from the measured discharging current and integrating it over time is known as Coulomb counting. This method, however, suffers from long-term drift and lack of a reference point. Therefore, the SoC should be calibrated on regular basis. Differentiating (1) with respect to t, we have

$$\dot{\mathrm{SoC}}(t) \quad = \quad -\frac{I(t)}{Q_c} \tag{2}$$

This model can be calibrated using measured terminal voltage. The terminal voltage can be obtained from the open circuit voltage (OCV), which underlying physical phenomenon of lithium-ion intercalation/deintercalation process and is expressed as a nonlinear function of the SoC. In practice, we create an OCV-SoC curve from experiments and use it as a lookup table for the model. An example could be seen in Fig. 1.

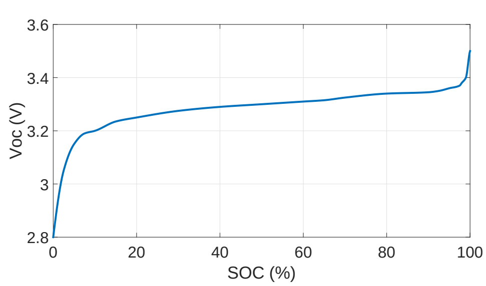

Fig. 1: A typical OCV-SoC lookup table for $LiFePO_4$ battery.

Using the OCV-SoC lookup table and the ECM (Fig. 2), the terminal voltage V can be calculated using the following formula

$$V(t) \quad = \quad V_{oc}(\mathrm{SoC}) - I(t)R - C(t) \tag{3}$$

where R is the internal resistance or the ohmic resistance. This ohmic resistance is used to represent the electrical resistance of battery components with the accumulation and dissipation of charge in the electrical double-layer. We assume V_{oc} is a continuously differentiable function, i.e., $\dot{V}_{oc}(\mathrm{SoC})$ exists and continuous. Furthermore, it could be easily observed from Fig. 1, $\dot{V}_{oc}(\mathrm{SoC}) > 0, \forall \mathrm{SoC} \in [0, 100]$. Here, C is a correction factor due to model inaccuracy and environmental conditions, e.g., ambient temperature variations. Some authors use the resistor model [14] and consider the value of C as a function of ambient temperature, which could be determined using least-square fitting from experimental data. Other authors consider C as the ECM with 1-RC circuit [28], 2-RC circuit [29], and multiple-RC circuit [30]. It could be also determined using a combination of Thevenin-based ECM [31] with the hysteresis voltage dynamics [32], which offers a grasp of dynamic current-voltage characteristics and compensates the static current-voltage property.

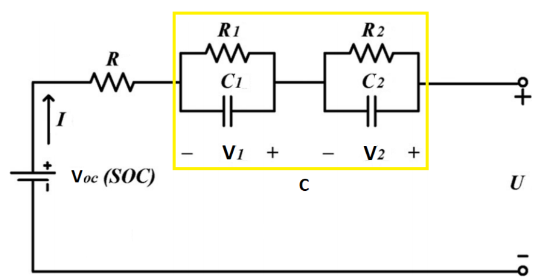

Fig. 2: Schematic diagram of the 2-RC circuit for $LiFePO_4$ battery.

To balance between the computational effort and accuracy, in this paper we use ECM with 2-RC circuit, i.e., $C(t) = V_1(t) + V_2(t)$, where

$$\dot{V}_1(t) \quad = \quad -\frac{V_1(t)}{R_1 C_1} + \frac{I(t)}{C_1} \tag{4}$$

$$\dot{V}_2(t) \quad = \quad -\frac{V_2(t)}{R_2 C_2} + \frac{I(t)}{C_2} \tag{5}$$

where R_1, R_2 and C_1, C_2 are diffusion resistances and diffusion capacitances for the RC network, respectively. These parameters could also be interpreted as the mass transport effects and dynamic voltage performance. These parameters together with the ohmic resistance could be determined from the exponential-function fitting method or a simple least-square algorithm [33].

III. SoC ESTIMATION USING EXOGENOUS KALMAN FILTER

Given the nonlinear battery model and measurements (2)-(5), the SoC estimation problem can be formulated as a nonlinear state estimation. A popular and natural choice for nonlinear state estimation is using Kalman filter-based methods, e.g., extended Kalman filter (EKF), Iterative EKF, and unscented Kalman filter (UKF), since they have the ability to suppress the noise affecting a battery system. Another method is using nonlinear observers, e.g., adaptive observer, sliding-mode observer, backstepping PDE observer, and robust nonlinear observer. These methods are relatively easy to implement and thus enables higher computational efficiency of SoC estimation.

The XKF is a cascade of a nonlinear observer and a linearized Kalman filter. The idea is to utilize each strength from both nonlinear state estimation methods, such as global stability properties from the nonlinear observer and noise elimination from the Kalman filter. The procedure is to use the exogenous state estimation obtained from the nonlinear observer to generate a linearized model for the Kalman filter, as can be seen from Fig. 3.

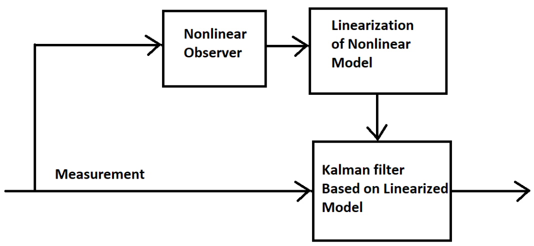

Fig. 3: The schematic diagram of the XKF.

A. State space model

From (2)-(5), the state-space model for the lithium-ion batteries is given by

$$\begin{pmatrix}\dot{V}_1(t)\\ \dot{V}_2(t)\\ \dot{\text{SoC}}(t)\end{pmatrix} = \begin{pmatrix}-\frac{1}{R_1C_1} & 0 & 0\\ 0 & -\frac{1}{R_2C_2} & 0\\ 0 & 0 & 0\end{pmatrix}\begin{pmatrix}V_1(t)\\ V_2(t)\\ \text{SoC}(t)\end{pmatrix} + \begin{pmatrix}\frac{1}{C_1}\\ \frac{1}{C_2}\\ -\frac{1}{Q_c}\end{pmatrix} I(t) \quad (6)$$

$$V(t) = V_{oc}(\text{SoC}) - V_1(t) - V_2(t) - RI(t) \quad (7)$$

To simplify the presentation, we can write (6)-(7) as follow

$$\dot{\mathbf{x}}(t) = \mathbf{A}\mathbf{x}(t) + \mathbf{B}I(t) \quad (8)$$

$$V(t) = h(\mathbf{x}) - RI(t) \quad (9)$$

where

$$\mathbf{x}(t) = \begin{pmatrix}V_1(t)\\ V_2(t)\\ \text{SoC}(t)\end{pmatrix} \quad (10)$$

$$\mathbf{A} = \begin{pmatrix}-\frac{1}{R_1C_1} & 0 & 0\\ 0 & -\frac{1}{R_2C_2} & 0\\ 0 & 0 & 0\end{pmatrix}, \mathbf{B} = \begin{pmatrix}\frac{1}{C_1}\\ \frac{1}{C_2}\\ -\frac{1}{Q_c}\end{pmatrix} \quad (11)$$

$$h(\mathbf{x}) = V_{oc}(\text{SoC}(t)) - V_1(t) - V_2(t) \quad (12)$$

To incorporate the model and measurement uncertainties and inaccuracies, noises are added into (8)-(9), thus the complete model becomes

$$\dot{\mathbf{x}}(t) = \mathbf{A}\mathbf{x}(t) + \mathbf{B}I(t) + w(t) \quad (13)$$

$$V(t) = h(\mathbf{x}) - RI(t) + v(t) \quad (14)$$

$$w \sim (0, \mathbf{Q}_n) \quad (15)$$

$$v \sim (0, \mathbf{R}_n) \quad (16)$$

where w denotes the process noise, $\mathbf{Q}_n$ is the process noise covariance, v is the measurement noise, and $\mathbf{R}_n$ is the measurement noise covariance. The values of $\mathbf{Q}_n$ and $\mathbf{R}_n$ can be obtained using Bayesian, maximum likelihood, covariance matching, and correlation techniques [34]. Note that the linear Kalman filter is optimal under the assumption that the model perfectly matches the real system, the noise w and v are white and uncorrelated, and the covariances of the noise $\mathbf{Q}_n$ and $\mathbf{R}_n$ are known. In this section, we design the nonlinear observer and the linearized Kalman filter for the XKF.

B. Nonlinear observer

The nonlinear observer is designed as follow

$$\dot{\overline{\mathbf{x}}}(t) = \mathbf{A}\overline{\mathbf{x}}(t) + \mathbf{B}I(t) + \mathbf{K}\left(V(t) - \overline{V}(t)\right) \quad (17)$$

$$\overline{V}(t) = h(\overline{\mathbf{x}}) - RI(t) \quad (18)$$

where $\overline{\mathbf{x}}$ denotes the exogenous state estimation from the nonlinear observer and $\mathbf{K} = \begin{pmatrix}k_1 & k_2 & k_3\end{pmatrix}^{\mathsf{T}} \in \mathbb{R}^3$ is the observer gain.

Lemma 1: If the nonlinear function h in (18) is Lipschitz and if we choose the gain $\mathbf{K} = \begin{pmatrix}0 & 0 & k_3\end{pmatrix}^{\mathsf{T}}$ where $k_3 > 0$, then the nonlinear observer (17)-(18) is globally exponentially stable.

Proof: Let us define $\breve{\mathbf{x}}(t) = \mathbf{x}(t) - \overline{\mathbf{x}}(t)$ and $\breve{V}(t) = V(t) - \overline{V}(t)$, then we have

$$\dot{\breve{\mathbf{x}}}(t) = \mathbf{A}\breve{\mathbf{x}}(t) - \mathbf{K}\breve{V}(t) \quad (19)$$

$$\breve{V}(t) = h(\mathbf{x}) - h(\overline{\mathbf{x}}) \quad (20)$$

Utilizing the smoothness property of the OCV-SoC lookup table, we can linearize the nonlinear measurement equation (20) using the mean value theorem. First, we write

$$\breve{V}(t) = -\breve{V}_1(t) - \breve{V}_2(t) + V_{oc}(\text{SoC}) - V_{oc}(\overline{\text{SoC}}) \quad (21)$$

Since h is Lipschitz, using the mean value theorem there exists $\text{SoC} \leq \xi \leq \overline{\text{SoC}}$, such that

$$V_{oc}(\text{SoC}) - V_{oc}(\overline{\text{SoC}}) = \dot{V}_{oc}(\xi)\breve{\text{SoC}}(t) \quad (22)$$

where $\dot{V}_{oc}(\xi) > 0$. Let us denote $\mathbf{T} = \begin{pmatrix}-1 & -1 & \dot{V}_{oc}(\xi)\end{pmatrix}$. Thus, we can write

$$\breve{V}(t) = \mathbf{T}\breve{\mathbf{x}}(t) \quad (23)$$

and the error equation becomes

$$\dot{\breve{\mathbf{x}}}(t) = (\mathbf{A} - \mathbf{K}\mathbf{T})\,\breve{\mathbf{x}}(t) \quad (24)$$

Note $\mathbf{T}$ is time-varying and bounded. In this particular case, let $k_1 = k_2 = 0$. Then, $\breve{V}_1(t) = \breve{V}_1(0)e^{-\frac{1}{R_1C_1}}$ and $\breve{V}_2(t) = \breve{V}_2(0)e^{-\frac{1}{R_2C_2}}$, i.e., $\breve{V}_1(t)$ and $\breve{V}_2(t)$ are exponentially stable. Correspondingly, we have $\dot{\breve{\text{SoC}}}(t) = -k_3\frac{\mathrm{d}V_{oc}}{\mathrm{dSoC}}(\xi)\breve{\text{SoC}}(t)$. Thus, if $k_3 > 0$ then the nonlinear observer is globally exponentially stable, i.e., the error will decay to zero and the estimate $\overline{\mathbf{x}}$ will converge to the actual value exponentially. ■

C. Linearized Kalman filter

Now we have $\overline{\mathbf{x}}$ as an estimate of $\mathbf{x}$, which is a bounded signal given by the nonlinear observer (17)-(18). We use this signal as an exogenous signal for the linearized Kalman filter. A first-order Taylor series expansion about the trajectory $\overline{\mathbf{x}}$ gives

$$\dot{\mathbf{x}}(t) = \mathbf{A}\mathbf{x}(t) + \mathbf{B}I(t) + w(t) \quad (25)$$

$$V(t) = h(\overline{\mathbf{x}}) + \mathbf{H}(\overline{\mathbf{x}})\check{\mathbf{x}} + r(\mathbf{x}, \overline{\mathbf{x}}) - RI(t) + v(t) \quad (26)$$

where

$$\mathbf{H}(\overline{\mathbf{x}}) = \frac{\partial h}{\partial \mathbf{x}}(\overline{\mathbf{x}}) = \begin{pmatrix} -1 & -1 & \frac{\partial V_{oc}(\text{SoC})}{\partial \text{SoC}} \end{pmatrix} \quad (27)$$

Remark that, since $\overline{\mathbf{x}}$ is bounded and converges to $\mathbf{x}$, we can neglect the higher-order term $r(\mathbf{x}, \overline{\mathbf{x}})$ since it has no consequences for stability. Thus, we can design the second stage estimator $\hat{\mathbf{x}}$ using the linearized Kalman filter as follow

$$\begin{aligned} \dot{\hat{\mathbf{x}}}(t) = {} & \mathbf{A}\hat{\mathbf{x}}(t) + \mathbf{B}I(t) \\ & + \mathbf{K}_K(t)\left(V(t) - h(\overline{\mathbf{x}}) - H(\overline{\mathbf{x}})(\hat{\mathbf{x}} - \overline{\mathbf{x}}) + RI(t)\right) \end{aligned} \quad (28)$$

The time-varying gain $\mathbf{K}_K(t)$ is given by

$$\mathbf{K}_K(t) = \mathbf{P}(t)\mathbf{H}^{\intercal}(\overline{\mathbf{x}})\mathbf{R}_n^{-1} \quad (29)$$

where $\mathbf{P}(t)$ is the solution to the Riccati equation

$$\dot{\mathbf{P}}(t) = \mathbf{A}\mathbf{P}(t) + \mathbf{P}(t)\mathbf{A}^{\intercal} + \mathbf{Q}_n - \mathbf{K}_K(t)\mathbf{R}_n\mathbf{K}_K^{\intercal}(t) \quad (30)$$

with $\mathbf{P}(0)$ symmetric and positive definite. Note that, unlike EKF, the XKF uses linear time-varying measurement model that is independent of the estimate $\hat{\mathbf{x}}$ in (28). To implement the algorithm with a discrete-time Kalman filter, the model has to be discretized, for example using the Euler discretization method. Following [27], the XKF result for SoC estimation is given as follow.

Lemma 2: Let $\tilde{\mathbf{x}} = \mathbf{x} - \hat{\mathbf{x}}$. The origin $\check{\mathbf{x}} = \tilde{\mathbf{x}} = 0$ of the unforced error dynamics cascade of the nonlinear observer (17)-(18) and the linearized Kalman filter (28) with $w = 0$ and $v = 0$ inherits the stability properties of the nonlinear observer (17)-(18).

IV. EVALUATION USING EXPERIMENTAL DATA

A $LiFePO_4$ battery is tested in two dynamic loading condition tests; the dynamic stress test (DST) and the federal urban driving schedule (FUDS). The DST was used to identify the model parameters, while the FUDS was used to validate the performance of the SoC estimation. The battery specification is given in TABLE I. A complete description regarding the tests is given in [14].

Type	Nominal voltage	Nominal capacity	Upper and lower cut-off voltage
$LiFePO_4$	3.3V	2.23Ah	3.6V and 2.0V

TABLE I: Battery specification.

To evaluate the validity and to identify the parameters of the battery model, the DST is run at 20°C. This test is designed by US Advanced Battery Consortium (USABC) to simulate a variable-power discharge regime that represents the expected demands of an electric vehicle (EV) battery. The voltage and current are measured and recorded from fully charged to empty with a sampling period of 1s based on the battery test bench. The accumulative charge was run continuously from 100% SOC at 3.6V to empty at 2V over several cycles in a discharge process. The measured current I and voltage V are given in Fig. 4. These measurements are used to calibrate the estimation from the Coulomb counting method.

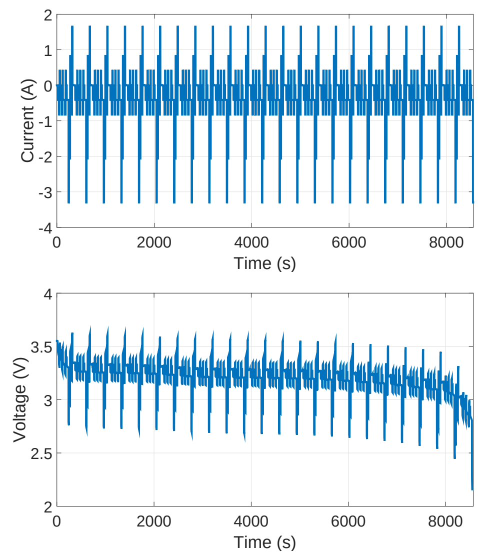

Fig. 4: Measured current and terminal voltage from dynamic stress test (DST).

The root mean square (RMS) error is used to evaluate the validity of the model and the parameters. The model parameters and the RMS error are given in TABLE II. Fig. 5 shows the fitting between the measured and estimated terminal voltage V and the error. A slight deviation can be observed when the voltage close to 2V, or when the SoC approach zero. This is due to inaccuracies when measuring the open circuit voltage. Notice that the diffusion resistance and the diffusion capacitance for V_1 and V_2 are equal, i.e., $V_1 = V_2$. The plots for V_1 and V_2 together with the estimated SoC are given in Fig. 6. The estimated SoC is used as a reference for the XKF.

R	R_1	C_1	R_2	C_2	RMS
0.18	0.035	1e6	0.035	1e6	8.4157e-05

TABLE II: Model parameters and RMS.

To test the proposed method, we run the simulation with initial SoC guess at 60% and compare it with some existing filter, e.g, EKF and UKF. The standard deviation for the process noise is 0.01, while for the measurement noise is 0.04. These values are obtained using a simple covariance matching technique. The initial error covariance matrix $\mathbf{P}(0)$

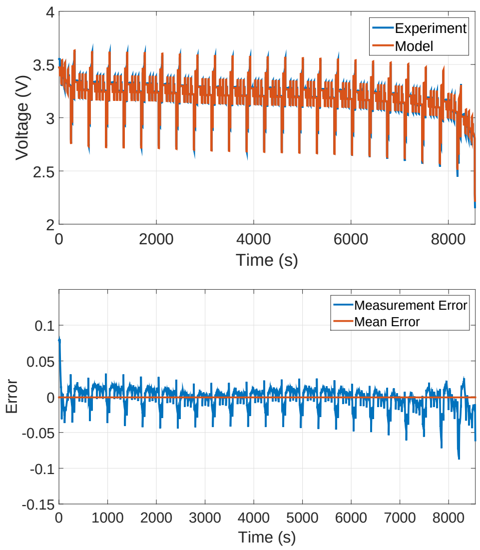

Fig. 5: The measured and the estimated voltage response on the DST profile and the model error.

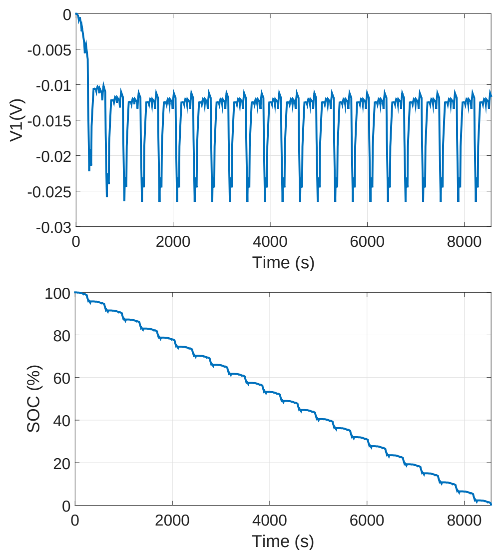

Fig. 6: The correction factor $V_1(t) = V_2(t)$ and the SoC.

is defined based on the initialization error. In this case, if the initial state is not very close, the value of $\mathbf{P}(0)$ should be large, whereas if the initialization is very good a smaller $\mathbf{P}(0)$ value can be used. The observer gain $k_3 = 1$. The results are given in Fig. 7. It could be observed that the nonlinear observer performs better in terms of the convergence rate than the EKF and UKF. The XKF improves the estimation further. The convergence rate can be increased using higher value of the gain k_3, as can be seen from Fig. 8. With $k_3 = 2$ the estimate converges to the actual value in one minutes, while with $k_3 = 0.5$, the estimate converges after almost one hour. However, keep in mind that higher observer tends to overshoot as can be seen between $t = 6500s$ to the end. Indeed, selecting an appropriate gain in crucial in SoC estimation. There is a trade-off between convergence rate and

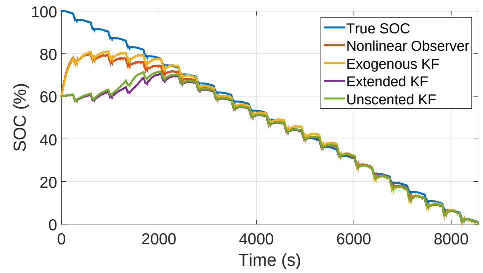

Fig. 7: The SoC estimation from different estimation methods for DST.

accuracy.

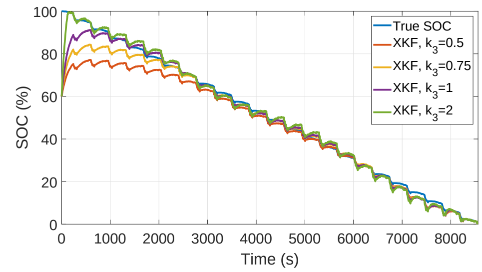

Fig. 8: Comparison of different observer gain k_3.

A more realistic dynamics current test is given by the FUDS test. FUDS is based on a time-velocity profile from an automobile industry standard vehicle to test the dynamic electric vehicle performance. The measured current and voltage can be seen in Fig. 9. The current profile causes variation of the SoC from fully charged at 3.6V to empty at 2V. We run the simulations from three different initial guesses. The results are given in Fig. 10. It can be observed that the estimation converges to the SoC for any initial guess.

V. CONCLUSIONS AND FUTURE WORKS

In this paper, we present SoC estimation of a $LiFePO_4$ battery using the XKF from the 2-RC ECM with Coulomb counting method. The estimation algorithm consists of a cascade of nonlinear observer and linearized Kalman filter. Simulations against experimental data from the dynamics stress test and federal urban driving schedule show the algorithm is able to estimate the SoC accurately. Furthermore, comparisons with existing filter show the estimation using XKF converges faster, thanks to the exponential stability from the nonlinear observer. Future work includes the use of thermal-electrochemical model to improve the lithium battery model.

REFERENCES

[1] G.E. Blomgren, The development and future of lithium-ion batteries, *Journal of The Electrochemical Society*, vol. 164, pp. A5019–A5025, 2017.

[2] R. Malik, A. Abdellahi, and G. Ceder, A critical review of the Li insertion mechanisms in $LiFePO_4$ electrodes, *Journal of The Electrochemical Society*, vol. 160, pp. A3179–A3197, 2013.

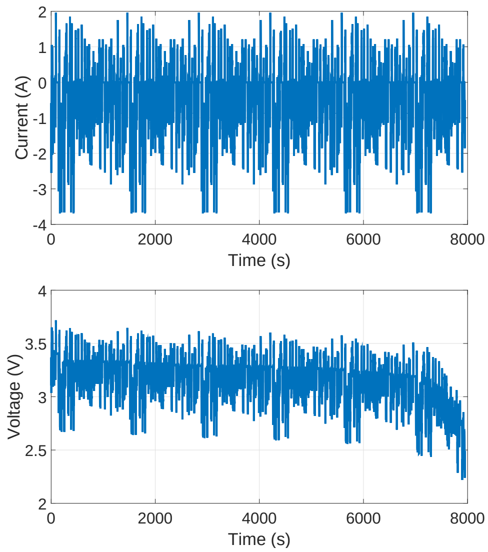

Fig. 9: Measured current and terminal voltage from federal urban driving schedule (FUDS).

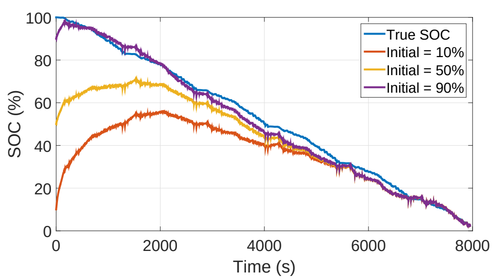

Fig. 10: The SoC estimation from XKF for FUDS.

[3] J.B. Goodenough and K.S. Park, The Li-ion rechargeable battery: a perspective, *Journal of The American Chemical Society*, vol. 135, pp. 1167–1176, 2013.

[4] S. Lee, J. Kim, J. Lee, B.H. Cho, State-of-charge and capacity estimation of lithium-ion battery using a new open-circuit voltage versus state-of-charge, *Journal of Power Sources*, vol. 185, pp. 1367–1373, 2008.

[5] S.J. Moura, F.B. Argomedo, R. Klein, A. Mirtabatabaei, and M. Krstic, Battery state estimation for a single particle model with electrolyte dynamics, *IEEE Transactions on Control Systems Technology*, vol. 25, pp. 453–468, 2017.

[6] A. Hasan and J. Jouffroy, Infinite-dimensional boundary observer for lithium-ion battery state estimation, *Energy Procedia*, vol. 141, pp. 494–501, 2017.

[7] S.-X. Tang, L. Camacho-Solorio, Y. Wang, and M. Krstic, State-of-Charge estimation from a thermal-electrochemical model of lithium-ion batteries, *Automatica*, vol. 83, pp. 206–219, 2017.

[8] M. Doyle, T.F. Fuller, and J. Newman, Modeling of galvanostatic charge and discharge of the lithium/polymer/insertion cell, *Journal of the Electrochemical Society*, vol. 140, pp. 1526–1533, 1993.

[9] S. Santhanagopalan, Q. Guo, P. Ramadass, and R. E. White, Review of models for predicting the cycling performance of lithium ion batteries, *Journal of Power Sources*, vol. 156, pp. 620–628, 2006.

[10] A. Hasan, O.M. Aamo, and M. Krstic, Boundary observer design for hyperbolic PDE-ODE cascade systems, *Automatica*, vol. 68, pp. 75–86, 2016.

[11] A. Hasan, L. Imsland, and E. Hauge, Design and experimental validation of nonlinear infinite-dimensional adaptive observer in automated managed pressure drilling, *Journal of Dynamic Systems, Measurement, and Control*, vol. 139, 2017.

[12] A. Hasan, "Adaptive boundary observer for nonlinear hyperbolic systems: Design and field testing in managed pressure drilling", *American Control Conference*, Chicago, USA, 2015.

[13] A. Hasan, "Adaptive boundary control and observer of linear hyperbolic systems with application to Managed Pressure Drilling", *ASME Dynamic Systems and Control Conference*, San Antonio, USA, 2014.

[14] Y. Xing, W. He, M. Pecht, and K.L. Tsui, State of charge estimation of lithium-ion batteries using the open-circuit voltage at various ambient temperatures, *Applied Energy*, vol. 113, pp. 106–115, 2014.

[15] A. Hasan and L. Imsland, "Moving horizon estimation in managed pressure drilling using distributed models", *IEEE Conference on Control Application*, Antibes, France, 2014.

[16] W. He, N. Williard, C. Chen, and M. Pecht, State of charge estimation for Li-ion batteries using neural network modeling and unscented Kalman filter-based error cancellation, *Electrical Power and Energy Systems*, vol. 62, pp. 783–791, 2014.

[17] X. Hu, S.E. Li, Y. Yang, Advanced machine learning approach for lithium-ion battery state estimation in electric vehicles, *IEEE Transactions on Transportation Electrification*, vol. 2, pp. 140–149, 2016.

[18] A. Hasan and T.A. Johansen, "Model-based actuator fault diagnosis in multirotor UAVs", *International Conference on Unmanned Aircraft Systems*, Dallas, USA, 2018.

[19] S.J. Moura, N.A. Chaturvedi, and M. Krstic, Adaptive partial differential equation Observer for battery state-of-charge/state-of-health estimation via an electrochemical model, *Journal of Dynamic Systems, Measurement, and Control*, vol. 136, 2014.

[20] Y. Wang, H. Fang, L. Zhou, and T. Wada, Revisiting the state-of-charge estimation for lithium-Ion batteries: A methodical investigation of the extended Kalman filter approach, *IEEE Control Systems Magazine*, vol. 37, 2017.

[21] W. He, N. Williard, C. Chen, and M. Pecht, State of charge estimation for electric vehicle batteries using unscented kalman filtering, *Microelectronics Reliability*, vol. 53, pp. 840–847, 2013.

[22] Y. Zou, X. Hu, H. Ma, and S.E. Li, Combined state of charge and state of health estimation over lithium-ion battery cell cycle lifespan for electric vehicles, *Journal of Power Sources*, vol. 273, pp. 793–803, 2015.

[23] B. Xia, C. Chen, Y. Tian, W. Sun, Z. Xu, and W. Zheng, A novel method for state of charge estimation of lithium-ion batteries using a nonlinear observer, *Journal of Power Sources*, vol. 270, pp. 359–366, 2014.

[24] J. Xu, C.C. Mi, B. Cao, J. Deng, Z. Chen, and S. Li, The state of charge estimation of lithium-ion batteries based on a proportional-integral observer, *IEEE Transactions on Vehicular Technology*, vol. 63, pp. 1614–1621, 2014.

[25] S. Dey and B. Ayalew, "Nonlinear observer designs for state-of-charge estimation of lithium-ion batteries", *American Control Conference*, Portland, USA, 2014.

[26] Q. Ouyang, J. Chen, F. Wang, and H. Su, "Nonlinear observer design for the state of charge of lithium-Ion batteries", *IFAC World Congress*, Cape Town, South Africa, 2014.

[27] T.A. Johansen and T.I. Fossen, The eXogenous Kalman Filter (XKF), *International Journal of Control*, vol. 90, pp. 161–167, 2017.

[28] X. Hu, S. Li, and H. Peng, A comparative study of equivalent circuit models for Li-ion batteries, *Journal of Power Sources*, vol. 198, pp. 359–367, 2012.

[29] X. Chen, W. Shen, Z. Cao, and A. Kapoor, A novel approach for state of charge estimation based on adaptive switching gain sliding mode observer in electric vehicles, *Journal of Power Sources*, vol. 246, pp. 667–678, 2014.

[30] J. Lee, O. Nam, and B.H. Cho, Li-ion battery SoC estimation method based on the reduced order extended Kalman filtering, *Journal of Power Sources*, vol. 174, pp. 9–15, 2007.

[31] M. Chen and G.A. Rincon-Mora, Accurate electrical battery model capable of predicting runtime and I-V performance, *IEEE Transactions on Energy Conversion*, vol. 31, pp. 504–511, 2006.

[32] G.L. Plett, Extended Kalman filtering for battery management systems of LiPB-based HEV battery packs: Part 2. Modeling and identification, *Journal of Power Sources*, vol. 134, pp. 262–276, 2004.

[33] W. Waag, S. Kabitz, and D.U. Sauer, Experimental investigation of the lithium-ion battery impedance characteristic at various conditions and aging states and its influence on the application, *Applied Energy*, vol. 102, pp. 885–897, 2003.

[34] B.J. Odelson, M.R. Rajamani, and J.B. Rawlings, A new autocovariance least-squares method for estimating noise covariances, *Automatica*, vol. 42, pp. 303–308, 2006.